Multi-Frequency Multi-Power One-to-Many Wireless Power Transfer System

Wei Liu[1], K.T. Chau[1], *Fellow*, *IEEE*, Christopher H.T. Lee[1, 2], *Senior Member*, *IEEE*, Chaoqiang Jiang[1], Wei Han[1] and W.H. Lam[1], *Senior Member*, *IEEE*

[1]Department of Electrical and Electronic Engineering, The University of Hong Kong, Hong Kong, China
[2]Research Laboratory of Electronics, Massachusetts Institute of Technology, Cambridge, MA 02139 USA

This paper proposes and implements a novel multi-frequency multi-power wireless power transfer (MFMP-WPT) system based on one single transmitter for simultaneously and compatibly energizing multi-standard receivers. Generally, implementing a multi-frequency WPT often requires a compromise in system complexity, control difficulty, switching frequency or transmission efficiency. By using only a single transmitter with an artful inverter topology, the proposed MFMP-WPT system can effectively achieve multi-frequency multi-magnitude superposition and switching frequency reduction while maintaining the control fitness and convenience of square-wave generation with 50% duty cycle. Moreover, by switching at the fundamental frequency in a range of 80-130 kHz, the single transmitter becomes competent for one-to-many MFMP-WPT operation for diverse wireless power on-demands. Consequently, the fundamental and high-order harmonic wireless energies with multiple power levels can be respectively picked up by the multi-standard receivers, depending on their energy requirements. The experimental transmission and system efficiencies can reach 81.57% and 64.74% under MFMP-WPT, respectively. Theoretical analysis, computer simulation and experimental results are provided to verify the feasibility of the proposed MFMP-WPT system.

***Index Terms*—Multi-frequency multi-power, wireless power transfer, single transmitter, one-to-many.**

I. Introduction

EPOCH-MAKING developments in wireless power transfer (WPT) technologies have promoted the arrival of a new wireless charging era in various applications from the consumer electronics [1] and medical implantable devices [2], [3] to electric vehicles [4]-[7]. The wireless energy-accessing pattern can totally eliminate the messy wires and adaptors, hence achieving wireless charging for multiple electric devices. Moreover, it takes the merits of great convenience, safety and high efficiency as compared with the conventional plug-in charging pattern [8].

Unfortunately, within the field of wireless energy-accessing, some challenging issues have been emerged recently. One of the most intractable problems is the non-unified WPT standards. As a result, the WPT standard divergence inevitably causes the charging inconvenience for consumers and manufacturers. Although a single-transmitter-based WPT has been identified to simultaneously transmit wireless power for multiple loads at a consistent operating frequency between the transmitter and receivers [9], it still fails to concurrently satisfy the multi-frequency wireless power on-demands from diverse-standard receivers. A selective WPT for smart power distribution among multi-standard receivers has been investigated in [10]. Strictly speaking, however, it should be classified as a single-frequency WPT system, essentially not transferring diverse-standard wireless powers simultaneously.

For improving power transferring compatibility, studies of multi-mode wireless charging strategies using multi-frequency band have been extensively conducted in [1], [11] and [12]. For example, a GaN-based programmable pulse width modulation [1] in Fig. 1 (left) and a concurrent transmitter consisting of two independent transmitters [11] were proposed and implemented to support the dual-mode WPT operation. However, the corresponding implementation of modulation cannot reduce the dependence of high-performance switching devices. Additionally, some multi-standard WPT technologies have already been investigated and fruitful research results have been reported [13]-[15]. A scheme that amplifies both the fundamental and 3rd harmonic generated by a full-bridge inverter was proposed to implement the double-frequency WPT (DF-WPT) [13], but only two selected fundamental and 3rd frequencies cannot satisfy the diverse wireless power on-demands from multi-standard receivers. Although a multi-frequency superposition methodology [14] in Fig. 1 (right) and a multi-frequency drive configuration [15] have been proposed to achieve high-efficiency and flexibly targeted power distribution for multi-load WPT, the need of multiple inverters and multiple transformers does not improve upon the system complexity and control difficulty. Consequently, by simplifying a quadruple-resonant inverter into a single-resonant counterpart [16], the inverter efficiency can be improved while the size be reduced.

This paper will propose and implement a novel multi-frequency multi-power (MFMP) WPT system, which can superpose the multi-frequency multi-magnitude transmitter currents while still operating at low frequency. The proposed one-to-many MFMP-WPT technology is promising for various WPT-based applications desiring high WPT-standard compatibility, such as public park-charging lots [17], [18], dynamic-charging roadways [19], [20], or universal wireless charging pads [10]. Meanwhile, it is practically attractive for simultaneously energizing both the armature winding and field winding in a wireless DC motor drive [21], or directly powering three-phase stator windings in a wireless AC motor drive [22].

Section II will discuss the multi-frequency multi-magnitude superposition methodology and multi-power characteristics of the proposed MFMP-WPT system. Section III will be devoted

to the computational simulation of electromagnetic fields and system circuit. In Section IV, an experimental prototype will be constructed and tested to verify the proposed system. A conclusion will be drawn in Section V.

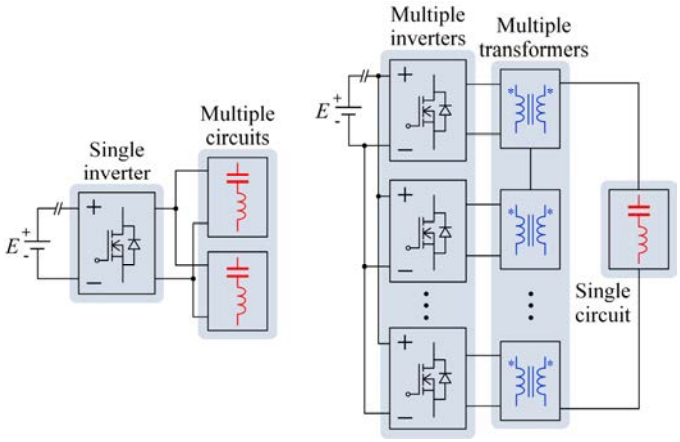

Fig. 1. Two conventional implementations of multi-frequency transmitter.

II. Multi-Frequency Multi-Power WPT System

By eliminating the messy charging wires and various adaptors, the one-to-many MFMP-WPT is a promising wireless energy-accessing pattern. It exhibits a strong compatibility on improving charging convenience in the multi-standard WPT-based applications, such as consumer electronics and medical implantable devices. Fig. 2 depicts the proposed one-to-many MFMP-WPT system based on a single transmitter – single inverter and single transmitter coil. The whole system mainly comprises of one transmitter and multi-standard receivers with diverse requirements on both the operating frequency and wireless power level. By introducing the multi-frequency multi-magnitude superposition methodology, the proposed MFMP-WPT system takes the definite merits of employing single transmitter and maintaining low operating frequency to simultaneously support wireless power on-demands for the multi-standard receivers.

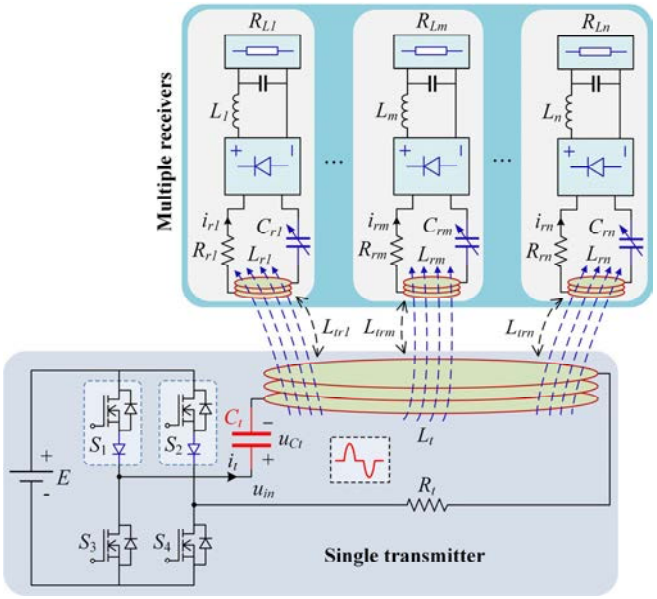

Fig. 2. Proposed MFMP-WPT system using single transmitter.

In Fig. 2, R_t, L_t, C_t, i_t, R_{rk}, L_{rk}, C_{rk} and i_{rk} ($k \in Z^+$) with subscripts t and r denote the coil internal resistances, resonant coil inductances, matched capacitances and resonant currents of the transmitter and receiver circuits in the k-th energy-accessing channel, respectively. Besides, L_{trk} and $L_{rk_1k_2}$ (k_1, $k_2 \in Z^+$) denote the mutual inductances between the transmitter and k-th receiver coils and that between the k_1-th and k_2-th receiver coils, respectively. To commence with theoretical analysis, some assumptions are made:

(i) $L_{rk}=L_r$, $L_{trk}=L_{tr}$, $R_{rk}=R_r$, and $R_{Lk}=R_L$.

(ii) R'_{Lk} is the equivalent resistance of load resistance R_{Lk}, and $R'_{Lk} = R_L$.

(iii) $L_{trk} >> L_{rk_1k_2}$, and $L_{rk_1k_2} \simeq 0$.

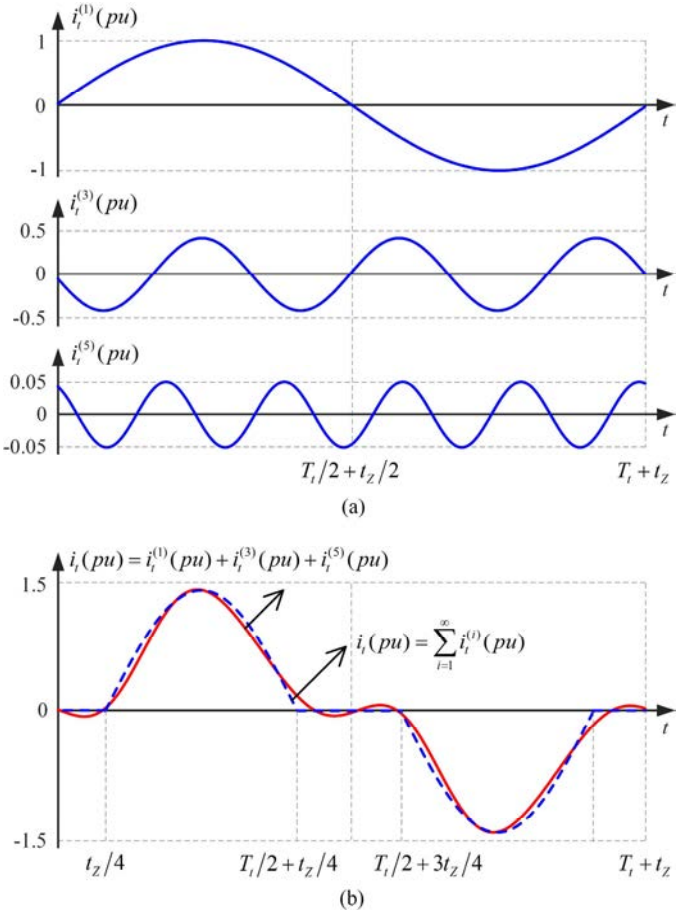

Fig. 3. Multi-frequency multi-magnitude superposition methodology. (a) Superposed fundamental and harmonic currents. (b) Synthetic transmitter current.

A. Multi-Frequency Multi-Magnitude Superposition

The multi-frequency multi-magnitude superposition methodology is illustrated in Fig. 3, where denotation i_t with superscript (i) represents the superposed i-th order fundamental or harmonic current. Notably, a synthetic half-cycle sinusoidal transmitter current can be derived by applying the superposition methodology of the specific fundamental, 3rd and 5th harmonic currents, namely the multi-frequency multi-magnitude superposition. Theoretically, superposing more high-order harmonics will effectively facilitate to construct an ideally half-cycle sinusoidal transmitter current as expressed by:

$$i_t(t)=\begin{cases}0,\ t\in R_{\text{zero}}\\ A_t\sin\left(\omega_t\left(t-t_Z/4\right)\right),\ t\in\left[t_Z/4,T_t/2+t_Z/4\right]\\ A_t\sin\left(\omega_t\left(t-3t_Z/4\right)\right),\ t\in\left[T_t/2+3t_Z/4,T_t+3t_Z/4\right]\end{cases} \tag{1}$$

where R_{zero} is the interval in which i_t=0 as shown in Fig. 3, and t_Z is the duration of R_{zero} during one switching period. Besides, A_t, T_t and ω_t are the magnitude, period and angular frequency of the half-cycle sinusoidal transmitter current. Due to the odd function characteristic of its periodic extension, $i_t(t)$ is only superposed by odd harmonic components.

By connecting one diode in series to each inverter leg as shown in Fig. 2, an artful inverter topology is introduced to practically implement the proposed superposition methodology. Only switching at the fundamental frequency but resonating at its inherent frequency, the single transmitter can approximately generate a half-cycle sinusoidal current as expressed in (1), which is actually the transmitter's resonant current. Thus, it can competently transmit both the fundamental and even high-order harmonic wireless powers. Moreover, the proposed MFMP-WPT system retains the merit of control applicability and convenience of square-wave generation possessed by conventional WPT systems. Most importantly, the fundamental and the harmonics can be arbitrarily selected as outputs for simultaneously energizing the multi-standard receivers.

Under the MFMP-WPT, all denotations with superscript (i) are corresponding to the i-th order fundamental or harmonic components. For example, $\omega_t^{(1)}$ and $\omega_t^{(3)}$ are the fundamental and 3rd harmonic angular frequencies of i_t. Accordingly, the equivalent general equation [9] of the proposed one-to-many MFMP-WPT system can be derived as:

$$\begin{bmatrix} Z_t & Z_{tr1}^{(i)} & \cdots & Z_{trm}^{(i)} & \cdots & Z_{trn}^{(i)}\\ Z_{tr1}^{(i)} & Z_{r1}^{(i)} & \cdots & Z_{r1m}^{(i)} & \cdots & Z_{r1n}^{(i)}\\ \vdots & \vdots & \ddots & \vdots & \vdots & \vdots\\ Z_{trm}^{(i)} & Z_{r1m}^{(i)} & \cdots & Z_{rm}^{(i)} & \cdots & Z_{rmn}^{(i)}\\ \vdots & \vdots & \vdots & \vdots & \ddots & \vdots\\ Z_{trn}^{(i)} & Z_{r1n}^{(i)} & \cdots & Z_{rmn}^{(i)} & \cdots & Z_{rn}^{(i)}\end{bmatrix}\begin{bmatrix} i_t^{(i)}\\ i_{r1}^{(i)}\\ \vdots\\ i_{rm}^{(i)}\\ \vdots\\ i_{rn}^{(i)}\end{bmatrix}=\begin{bmatrix} U_{in}^{(i)}\\ 0\\ \vdots\\ 0\\ \vdots\\ 0\end{bmatrix} \tag{2}$$

where $Z_{trk}^{(i)}=j\omega_t^{(i)}L_{trk}$, $Z_{rk_1k_2}^{(i)}=j\omega_t^{(i)}L_{rk_1k_2}$ and denotation $U_{in}^{(i)}$ is the i-th order fundamental or harmonic root-mean-square (RMS) value of input voltage u_{in}. Since both the transmitter and specified receivers are operating at their inherent resonances, the transmitter impedance Z_t and the k-th receiver impedance $Z_{rk}^{(i)}$ can be respectively expressed as:

$$\begin{cases}Z_t=R_t+j\omega_tL_t+1/\left(j\omega_tC_t\right)=R_t\\ Z_{rk}^{(i)}=R_{Lk}'+R_{rk}+j\omega_t^{(i)}L_{rk}+1/\left(j\omega_t^{(i)}C_{rk}\right)\end{cases} \tag{3}$$

where the equivalent resistance can be calculated as $R_{Lk}'=8R_{Lk}/\pi^2$ [23] by neglecting the power losses and effects of the output smoothing components.

Under the exemplified DF-WPT, the m-th and 1st receivers are simultaneously specified to pick up the fundamental and 3rd harmonic wireless powers, respectively. It yields $Z_{rm}^{(1)}=R_{Lm}'+R_{rm}$ and $Z_{r1}^{(3)}=R_{L1}'+R_{r1}$.

Then, the input impedance angle φ, input power P_{in} and total output power P_{outk} in the k-th energy-accessing channel can be respectively derived as:

$$\begin{cases}\varphi^{(i)}=\arctan\left(\text{Im}\left(Z_t+Z_{ref}^{(i)}\right)/\text{Re}\left(Z_t+Z_{ref}^{(i)}\right)\right)\\ P_{in}^{(i)}=\left(U_{in}^{(i)}\right)^2/\left|Z_t+Z_{ref}^{(i)}\right|\cos\varphi\\ P_{outk}^{(i)}=\left|j\omega_t^{(i)}L_{trk}\,U_{in}^{(i)}/\left(Z_{rk}^{(i)}\left(Z_t+Z_{ref}^{(i)}\right)\right)\right|^2R_{Lk}'\end{cases} \tag{4}$$

where the total impedance Z_{ref} reflected from all the receivers can be calculated as:

$$Z_{ref}^{(i)}=\sum_{k=1,\,k\neq m}^{n}\frac{(\omega_t^{(i)}L_{trk})^2}{Z_{rk}^{(i)}} \tag{5}$$

Hence, the general expression of transmission efficiency in the k-th energy-accessing channel can be derived as:

$$\eta_k^{(i)}=\frac{P_{outk}^{(i)}}{P_{in}^{(i)}}=\frac{R_{Lk}'\left(\omega_t^{(i)}L_{psk}\right)^2}{\left|Z_{rk}^{(i)}\right|^2\left(\text{Re}\left(\sum_{k=1,}^{n}\frac{(\omega_t^{(i)}L_{trk})^2}{Z_{refk}^{(i)}}\right)+R_t\right)} \tag{6}$$

Particularly, the corresponding transmission efficiency at f_i (i=1, 3) can be expressed as:

$$\eta_q^{(i)}=\frac{R_L'}{R+\sum_{k=1,\,k\neq q}^{n}\frac{R^3}{R^2+\left(\omega_t^{(i)}L_r-1/\omega_t^{(i)}C_{rk}\right)^2}+\frac{R_tR^2}{\left(\omega_t^{(i)}L_{tr}\right)^2}} \tag{7}$$

where if q=m, i=1; if q=1, i=3. Besides, Re( ) is the real part of the complex impedance, and $R=R_L'+R_r$. By neglecting the effects of other high-order harmonics, the total transmission efficiency can be expressed as:

$$\eta_{total}\simeq\frac{P_{outm}^{(1)}+P_{outm}^{(3)}+P_{out1}^{(1)}+P_{out1}^{(3)}}{P_{in}^{(1)}+P_{in}^{(3)}}\simeq\eta_m+\eta_1 \tag{8}$$

According to (6)-(8), the transmission efficiencies are impervious to the transmitter's resonant parameters L_t and C_t.

B. Multi-Power WPT

Because of the odd function characteristic, the transmitter current i_t in (1) can be expressed as:

$$i_t(t)=A\cdot\sum_{n=1}^{\infty}\left[\frac{(-1)^{(n-1)}\cos\left[(2n-1)\omega_t^{(1)}T_t/4\right]}{\omega_t^2-\left[(2n-1)\omega_t^{(1)}\right]^2}\sin\left[(2n-1)\omega_t^{(1)}t\right]\right] \tag{9}$$

where $A=8A_t\omega_t\omega_t^{(1)}/(2\pi)$, which only consists of the fundamental and odd-order harmonic currents. Thus, the Fourier series of (9) can further confirm the nature of multi-frequency multi-magnitude superposition.

Setting the transmitter's resonant frequency f_t and the superposed fundamental current magnitude as the baseline values of operating frequency and magnitude, respectively, Fig. 4 demonstrates the calculated magnitudes of the fundamental, 3rd, 5th and 7th harmonics versus different operating frequencies. It can be observed that the 3rd harmonic magnitude as well as the corresponding 3rd harmonic wireless power will monotonically increase with the decrease of operating frequency. Moreover, at points (f_a, 0.471), (f_b, 0.333) and (f_c, 0.235), the wireless power transmission ratios between the

fundamental and 3rd harmonics can be appropriately regulated at 2:1, 1:1 and 1:2, respectively. Thus, the high-magnitude fundamental and 3rd harmonic components can be selected for low-frequency high-power WPT. Meanwhile, the low-magnitude 5th and 7th harmonics can be utilized for the high-frequency low-power WPT. Accordingly, the MFMP-WPT system can select the superposed multi-frequency multi-magnitude transmitter current as wireless power outputs, and even the power distribution among different receivers can be artificially determined. Therefore, the distinct harmonic magnitudes successfully facilitate the proposed system to be competent for the MFMP-WPT operation with multi-standard receivers.

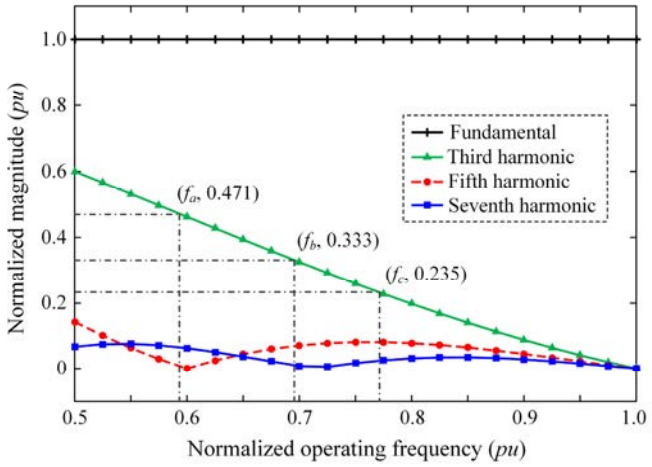

Fig. 4. Normalized magnitudes of the fundamental and the harmonics.

III. Computational Simulation

To assess the feasibility of the proposed MFMP-WPT system using a single transmitter, finite element analysis (FEA) and system simulation are performed. The key design specifications and parameters are listed in Table I. Detailed geometries with dimensions of the single-layer transmitter and three-layer receiver coils are depicted in Fig. 5, where all the receiver coils adopt a three-layer configuration to enhance mutual inductances between the transmitter and receiver coils, hence improving the transmission efficiency. The transmission distance is 105 mm and each receiver coil can respectively pick up the on-demand multi-standard wireless power.

TABLE I
Design Specifications and Parameters

Items	Values
DC input voltage (E)	55 V
Transmitter matched capacitance (C_t)	5.50 nF
Transmitter coil inductance (L_t)	204.20 μH
Transmitter coil internal resistance (R_t)	0.4 Ω
Transmitter resonant frequency (f_t)	150.180 kHz
Receiver l matched capacitance (C_{rl})	1.132~2.989 nF
Receiver m matched capacitance (C_{rm})	10.03~26.48 nF
Receiver n matched capacitance (C_{rn})	0.4045~1.068 nF
Receiver coil inductances (L_{rl}, L_{rm}, L_{rn})	147.13, 149.47, 148.21 μH
Receiver coil internal resistance (R_{rk})	0.2 Ω
Mutual inductances (L_{trl}, L_{trm}, L_{trn})	10.95, 11.33, 11.17 μH
Fundamental frequency (f_k)	80~130 kHz
Smoothing inductance (L_k)	5.0 μH
Load resistance (R_{Lk})	2.0 Ω

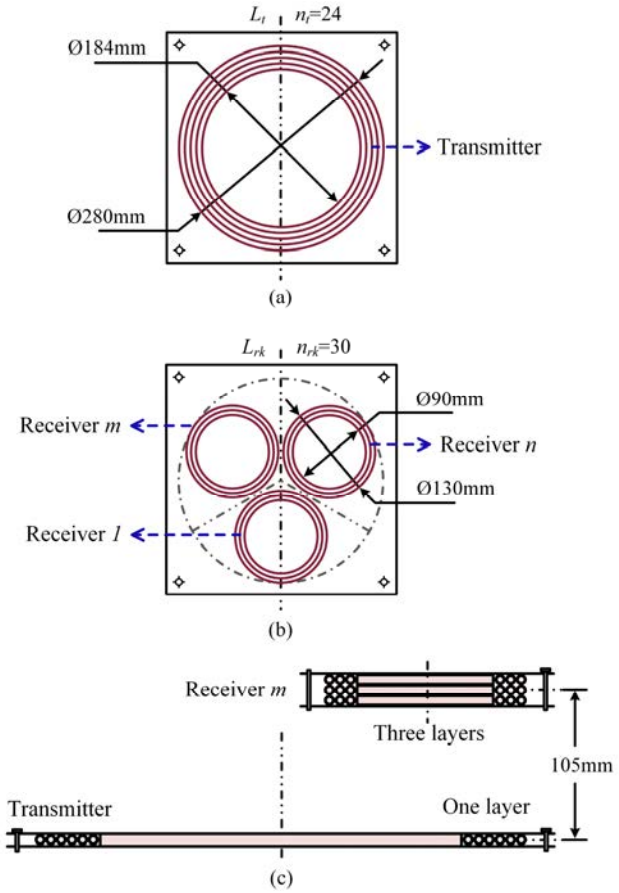

Fig. 5. Geometries of transmitter and receiver coils. (a) Transmitter coil. (b) Receiver coils. (c) Displacement among coils.

Operating at the frequency f_c as shown in Fig. 4, the corresponding fundamental, 3rd and 5th harmonic frequencies are 114.5 kHz, 343.5 kHz and 572.5 kHz with the magnitudes of 1, 0.235 and 0.0808, respectively. By using FEA, the magnetic field distributions at these three frequencies for simultaneous multi-frequency WPT are shown in Fig. 6 in which each receiver coil L_{rm}, L_{r1} or L_{rn} is permitted to harvest the specified one of the fundamental, 3rd or 5th harmonic wireless power, respectively. In Figs. 6(a)-(c), it can be observed that at each operating frequency, the magnetic flux channel is effectively built up in the proposed one-to-many MFMP-WPT system, and thus almost all of the magnetic flux lines are bundled up through the specified energy-harvesting receiver coil. Furthermore, the current densities in the specified energy-harvesting receiver coils can reach up to 5.5×10^5 A/m^2, 4.0×10^5 A/m^2 and 2.5×10^5 A/m^2, respectively, which are extremely higher than those in the unspecified ones. Meanwhile, the magnetic flux densities along the middle parallel plane are also depicted in Fig. 6, where the magnetic flux densities under the specified energy-harvesting receiver coil can rise up to 0.279 mT, 0.192 mT and 0.123 mT as shown in Figs. 6(d)-(f), respectively.

Moreover, under the exemplified DF-WPT operating at 100.73 kHz, Fig. 7(a) shows the simulation waveforms of the driving signal, transmitter' superposed current, resonant voltage and two receivers' induced currents. Notably, the transmitter's superposed current is ideally half-cycle sinusoidal due to the use of ideal power devices. In the three DF-WPT

cases of 85 kHz, 100.73 kHz and 114.5 kHz, Fig. 7(b) shows that the two specified energy-harvesting receivers can pick up the fundamental and 3rd wireless powers and generate various output voltage combinations (u_{o1}, u_{om}): (6.70 V, 5.05 V), (6.30 V, 6.28 V), and (5.53 V, 7.83 V), corresponding to the power transmission ratios of 1.760:1, 1.005:1 and 1:2.005, respectively. Under the exemplified triple-frequency WPT (TF-WPT) at 114.5 kHz, Fig. 7(c) demonstrates that the three specified energy-harvesting receivers can pick up the fundamental, 3rd and 5th wireless powers and generate the output voltages (u_{om}, u_{o1} and u_{on}) of 7.47 V, 4.96 V and 2.45 V, respectively.

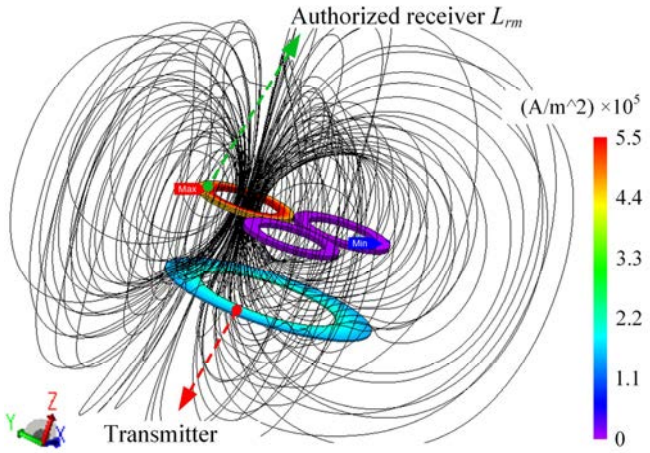

(a)

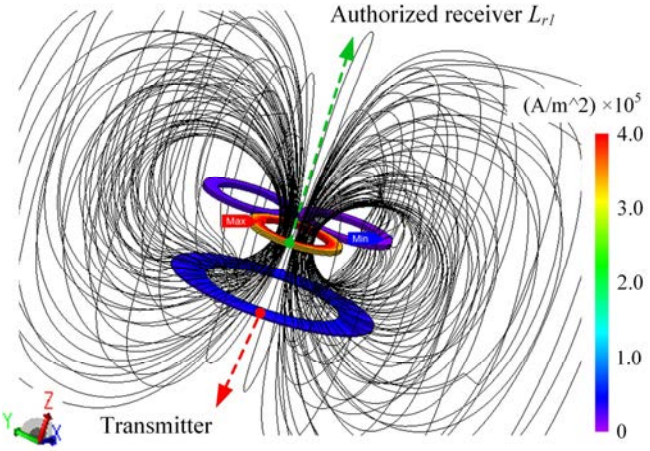

(b)

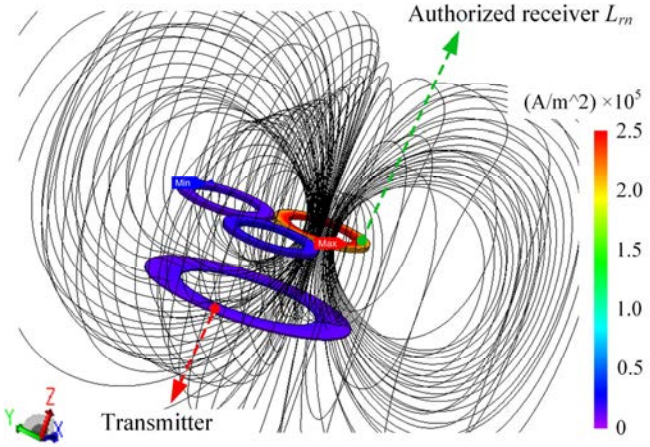

(c)

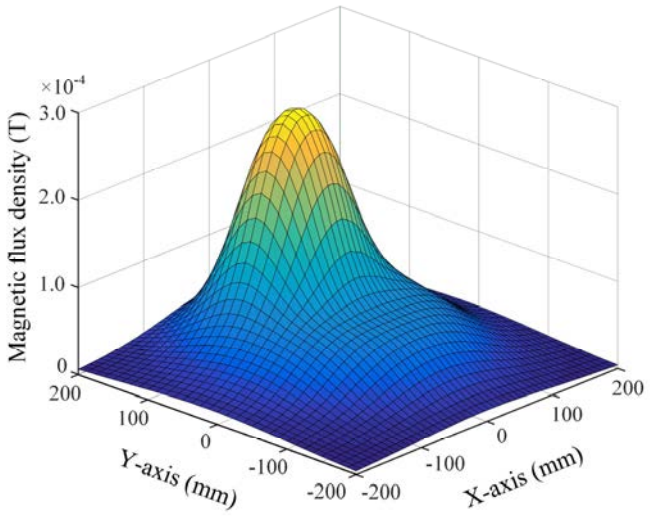

(d)

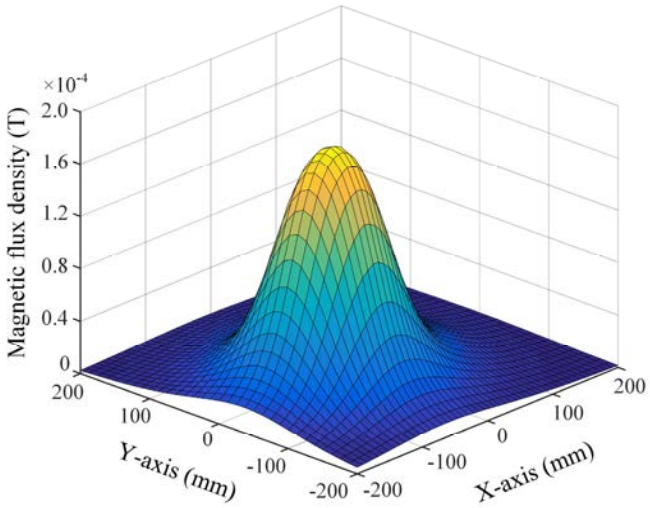

(e)

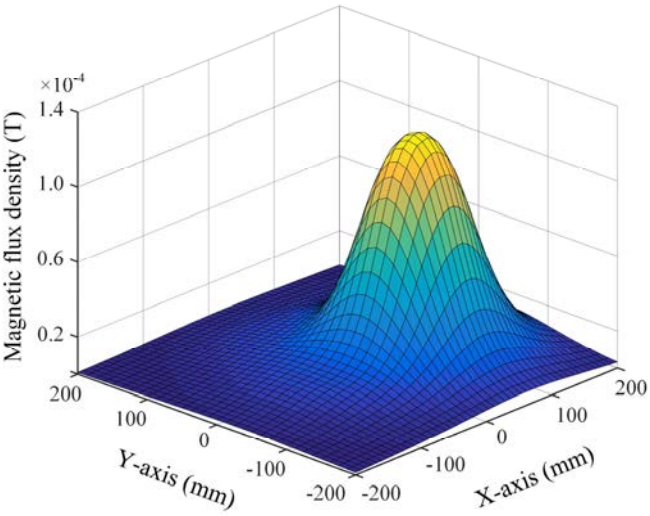

(d)

Fig. 6. Electromagnetic field distributions of proposed one-to-many MFMP-WPT system. (a) Flux lines and current densities (fundamental: 114.5 kHz). (b) Flux lines and current densities (3rd harmonic: 343.5 kHz). (c) Flux lines and current densities (5th harmonic: 572.5 kHz). (d) Flux densities (fundamental: 114.5 kHz). (e) Flux densities (3rd harmonic: 343.5 kHz). (f) Flux densities (5th harmonic: 572.5 kHz).

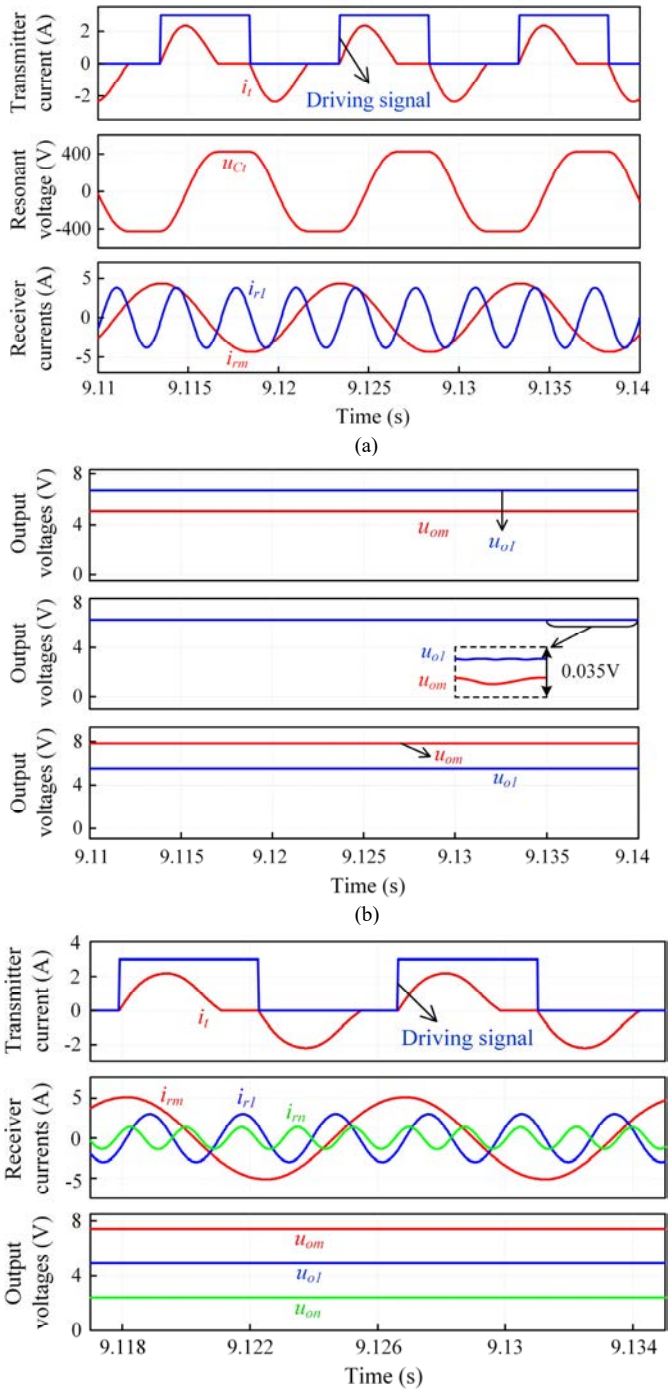

Fig. 7. Simulation waveforms of proposed one-to-many MFMP-WPT system. (a) Transmitter's and receivers' resonances under DF-WPT. (b) Output voltages at various operating frequencies under DF-WPT. (c) Transmitter's and receivers' resonances and output voltages under TF-WPT.

Finally, Figs. 8(a) and (b) demonstrate the receiving power distributions and coil-to-coil transmission efficiencies at different operating frequencies under the exemplified DF-WPT and TF-WPT, respectively. Under the DF-WPT, the decreasing trend of the harvested 3rd harmonic wireless power as well as the increasing trend of the harvested fundamental wireless power with the increasing operating frequency well agrees with the theoretical magnitude changes as shown in Fig. 4. Thus, the power distribution can be artificially determined by selecting an appropriate operating frequency. Furthermore, the relatively high transmission efficiency, always higher than 82.46%, increases with the increasing frequency. Under the TF-WPT, the fundamental and 3rd harmonic power distribution exhibits slight difference as compared with that under the DF-WPT, which is due to the effect of the 5th receiver load. Nevertheless, by selecting an appropriate operating frequency, it can also effectively regulate the power distribution. Moreover, the changing trend of the harvested 5th harmonic wireless power further confirms the theoretical analysis, and the transmission efficiency can keep higher than 81.87%.

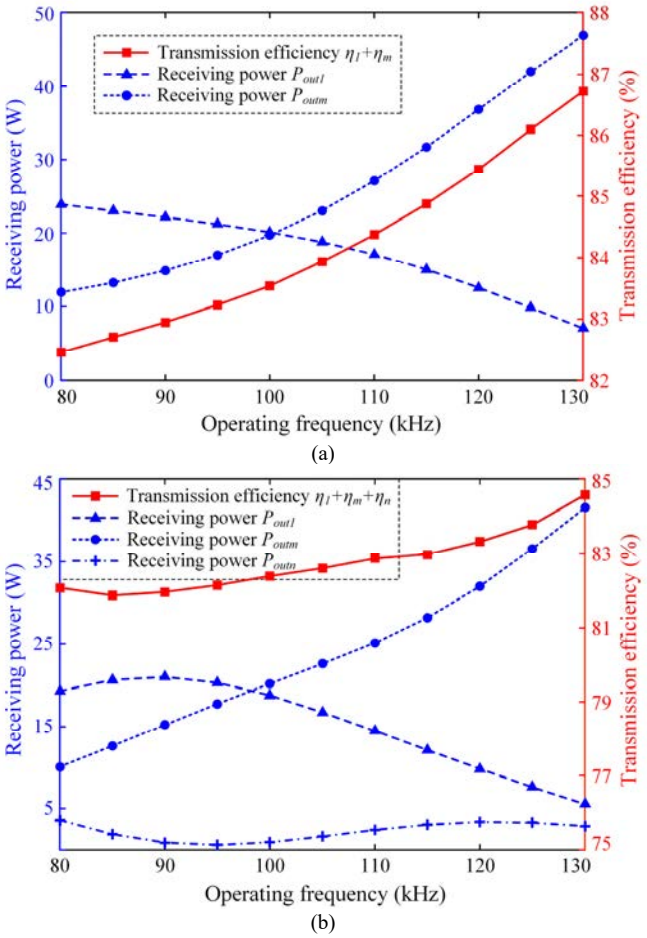

Fig. 8. Simulation characteristics of power distribution and transmission efficiency of proposed one-to-many MFMP-WPT system. (a) DF-WPT. (b) TF-WPT.

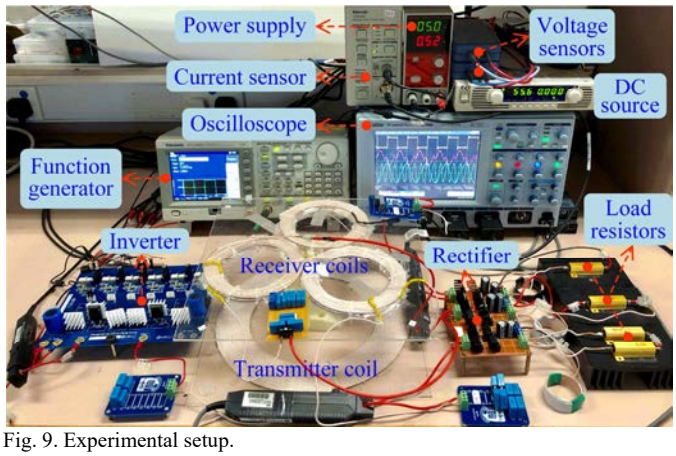

Fig. 9. Experimental setup.

IV. Experimental Verification

An exemplified prototype is built for experimental verification as shown in Fig. 9, where only one single transmitter is used for the MFMP-WPT. The driving signal is generated by an arbitrary/function generator (Tektronix AFG 3022C). For the sake of reducing the skin and proximity effects, litz wire (165×0.1 mm) is adopted for winding the transmitter and receiver coils. All voltage and current waveforms are measured by a storage oscilloscope (Lecroy 6100A).

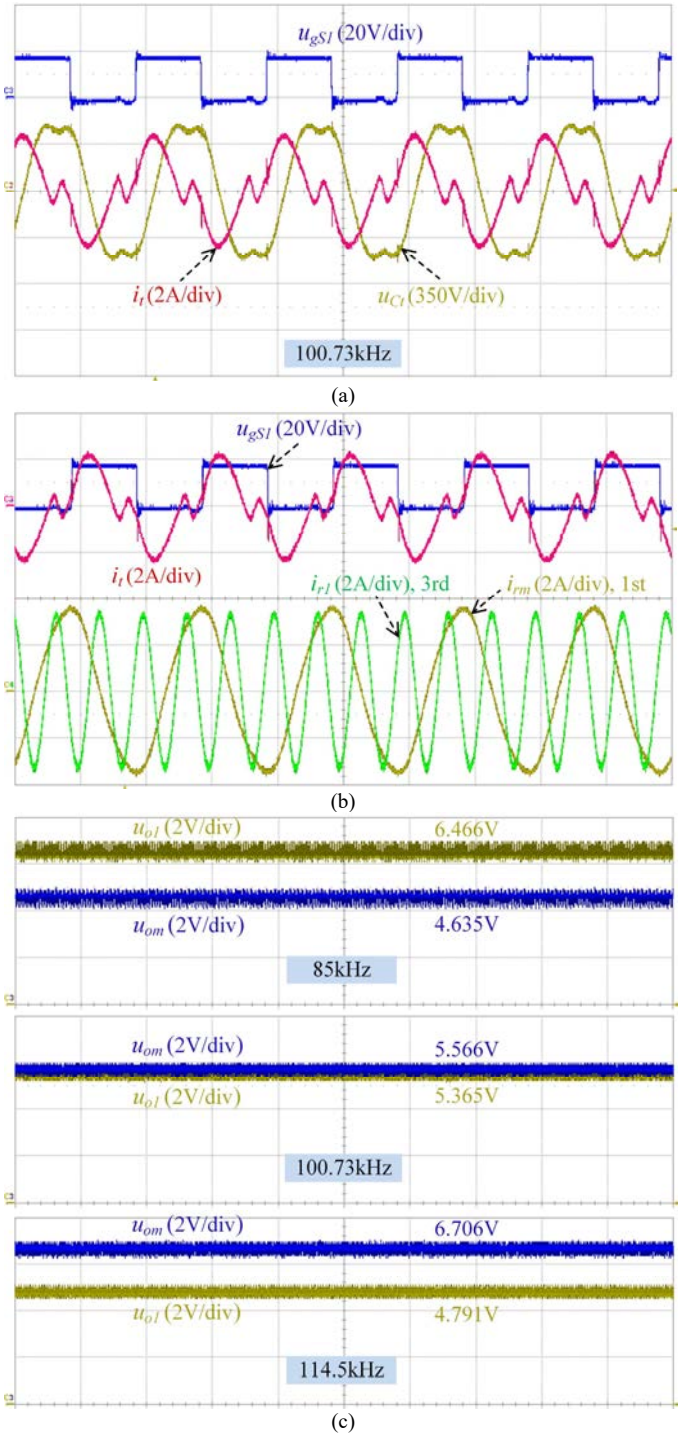

Fig. 10. Measured waveforms of proposed MFMP-WPT system under DF-WPT. (a) Driving signal, transmitter's superposed current and resonant voltage. (b) Transmitter's superposed current and receivers' currents. (c) Output voltages under various power distributions.

Under the exemplified DF-WPT, Fig. 10 shows the measured waveforms of the proposed MFMP-WPT system using a single transmitter. The driving signal u_{gs1} of switch S_1, transmitter's superposed current i_t and resonant voltage u_{Ct} across transmitter's fixed capacitor are measured at 100.73 kHz as shown in Fig. 10(a). Due to the inevitable reverse recovery and parasitic output capacitance of non-ideal power devices, the transmitter's current superposes slight ripples as compared with the ideally half-cycle sinusoidal one in Fig. 7 (a). Nevertheless, it well agrees with the theoretically synthetic one superposed by finite order harmonics in Fig. 3(b), and thus the multi-frequency currents are successfully synthesized by the single transmitter. Meanwhile, Fig. 10(b) shows that the single transmitter's superposed current can simultaneously excite two specified receivers to generate the fundamental and 3rd harmonic currents and thus to pick up the fundamental and 3rd harmonic wireless powers, respectively. At the exemplified frequencies of 85 kHz, 100.73 kHz and 114.5 kHz as labeled in Fig. 4, Fig. 10(b) shows that the two specified receivers can harvest the fundamental and 3rd wireless powers and generate various output voltage combinations (u_{o1}, u_{om}): (6.466 V, 4.635 V), (5.566 V, 5.365 V), and (6.706 V, 4.791 V), corresponding to the power transmission ratios of 1.946:1, 1.076:1 and 1:1.959, respectively. Both the output voltages and targeted wireless power distributions are slightly different from the simulated ones as shown in Fig. 7(b), which can be attribute to the small ripples of transmitter's superposed current and the inevitable power losses in capacitors, contacts and rectifiers. Consequently, the measured waveforms in Fig. 10 well agree with both the theoretical analysis in Fig. 4 as well as the simulation results in Figs. 7 and 8.

Moreover, the measured waveforms of the proposed single-transmitter-based MFMP-WPT system under the TF-WPT operating at 114.5 kHz are shown in Fig. 11, where Fig. 11(a) demonstrates the measured driving signal, transmitter current and resonant voltage. Meanwhile, Fig. 11(b) shows that the single transmitter's superposed current can simultaneously energize three specified receivers and generate the fundamental, 3rd and 5th resonant currents, respectively. Notedly, the synthetic transmitter current also contains slight ripples, but it only leads to an insignificant effect on the power distribution under the proposed MFMP-WPT. Besides, both the measured waveforms and their corresponding zoom-in patterns of three receivers' output voltages as well as the transmitter's superposed current are shown in Fig. 11(c). It can be observed that the three energy-harvested receivers can pick up the fundamental, 3rd and 5th wireless powers from the single transmitter and generate 7.256 V, 4.780 V and 2.212 V, respectively. The measured waveforms well agree with the simulated ones in Fig. 7. Consequently, more wireless power distributions can be artificially regulated by selecting proper operating frequency according to the characteristics in Fig. 4.

Under the DF-WPT and TF-WPT, the measured transmission efficiencies of the proposed MFMP-WPT system using a single transmitter can reach 81.57% and 80.25%, respectively, though slightly lower than the simulated ones. In a meantime, its overall system efficiencies are 63.40% and 64.74%, respectively, relatively lower than the transmission efficiencies, which are actually due to the inevitable power losses along the

matched capacitors, lines, contacts and rectifiers. As compared with the selective multi-frequency WPT [10], [19], the proposed one-to-many MFMP-WPT system can achieve simultaneously energizing multi-receivers with different WPT standards. Also, it can flexibly conduct variable multi-frequency WPT for multi-standard wireless energy-on-demands from more than two receivers [13] with different power levels. Moreover, it consists of only one transmitter, namely single inverter and single transmitter resonant tank, rather than multiple transmitters involving multiple transmitter resonant circuits [1], multiple inverters [10] or multiple transformers [14], [15]. Additionally, the proposed one-to-many MFMP-WPT system always operates at low-frequency switching without high-frequency modulation [1], which can maintain the control fitness and convenience of square-wave generation.

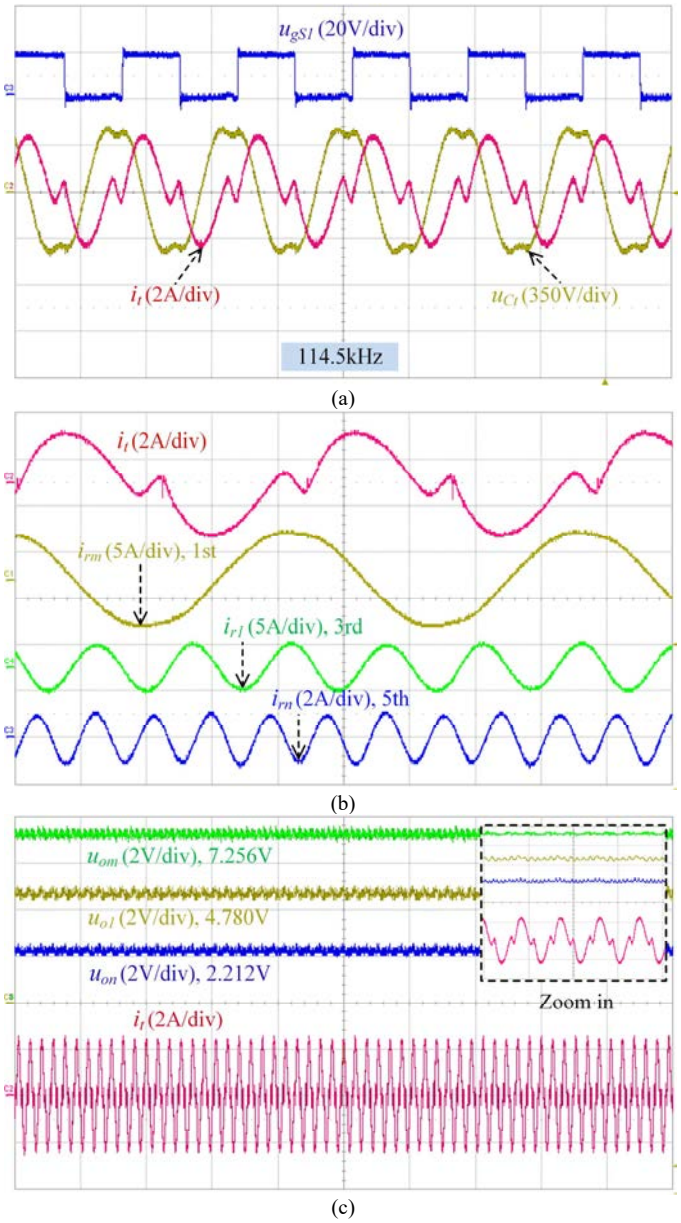

Fig. 11. Measured waveforms of proposed MFMP-WPT system under TF-WPT. (a) Driving signal, transmitter's superposed current and resonant voltage. (b) Transmitter's superposed current and receivers' currents. (c) Output voltages and transmitter's superposed current.

V. Conclusion

A novel one-to-many MFMP-WPT system using a single transmitter has been proposed and then implemented for diverse wireless power on-demands from various multi-standard receivers. The proposed single-transmitter-based MFMP-WPT system, switching at the low fundamental frequency in the range of 80-130 kHz, can achieve multi-frequency multi-magnitude superposition and thus one-to-many MFMP-WPT operation while maintaining the control fitness and convenience of square-wave generation. Consequently, the specified energy-harvesting multi-standard receivers can simultaneously pick up the diverse-frequency diverse-power wireless energies. Based on the exemplified prototype, the experimental transmission and system efficiencies can reach 81.57% and 64.74% under MFMP-WPT, respectively. The feasibility of the proposed one-to-many-MFMP-WPT system has been fully verified by theoretical analysis, simulation and experimentation.

Acknowledgment

This work was supported by a grant (Project No. 17204317) from the Hong Kong Research Grants Council, Hong Kong Special Administrative Region, China.

References

[1] C. Zhao and D. Costinett, "GaN-based dual-mode wireless power transfer using multifrequency programmed pulse width modulation," *IEEE Trans. Ind. Electron.*, vol. 64, no. 11, pp. 9165-9176, Nov. 2017.

[2] C. Liu, C. Jiang, J. Song and K. T. Chau, "An effective sandwiched wireless power transfer system for charging implantable cardiac pacemaker," *IEEE Trans. Ind. Electron.*, vol. 66, no. 5, pp. 4108-4117, May 2019.

[3] S. C. Tang, T. L. T. Lun, Z. Guo, K. Kwok and N. J. McDannold, "Intermediate range wireless power transfer with segmented coil transmitters for implantable heart pumps," *IEEE Trans. Power Electron.*, vol. 32, no. 5, pp. 3844-3857, May 2017.

[4] Z. Zhang, K. T. Chau, C. Liu, C. Qiu and F. Lin, "An efficient wireless power transfer system with security considerations for electric vehicle applications," *Journal of Applied Physics*, vol. 115, no. 17, paper no. 17A328, pp. 1-3, May 2014.

[5] Z. Zhang, K. T. Chau, C. Liu, C. Qiu, and T.W. Ching, "A positioning-tolerant wireless charging system for roadway-powered electric vehicles," *Journal of Applied Physics*, vol. 117, no. 17, paper no. 17B520, pp. 1-4, Mar. 2015.

[6] A. Kamineni, M. J. Neath, G. A. Covic and J. T. Boys, "A mistuning-tolerant and controllable power supply for roadway wireless power systems," *IEEE Trans. Power Electron.*, vol. 32, no. 9, pp. 6689-6699, Sep. 2017.

[7] C. Jiang, K. T. Chau, C. Liu, C. H. T. Lee, W. Han and W. Liu, "Move-and-charge system for automatic guided vehicles," *IEEE Trans. Magn.*, vol. 54, no. 11, pp. 8600105:1-5, Nov. 2018.

[8] Z. Zhang, H. Pang, A. Georgiadis and C. Cecati, "Wireless power transfer - an overview," *IEEE Trans. Ind. Electron.*, vol. 66, no. 2, pp. 1044-1058, Feb. 2019.

[9] W. Liu, K. T. Chau, C. H. T. Lee, C. Jiang and W. Han, "A switched-capacitorless energy-encrypted transmitter for roadway-charging electric vehicles." *IEEE Trans. Magn.*, vol. 54, no. 11, pp. 1-6, Nov. 2018.

[10] Y. J. Kim, D. Ha, W. J. Chappell and P. P. Irazoqui, "Selective wireless power transfer for smart power distribution in a miniature-sized multiple-receiver system," *IEEE Trans. Ind. Electron.*, vol. 63, no. 3, pp. 1853-1862, Mar. 2016.

[11] D. Ahn and P. P. Mercier, "Wireless power transfer with concurrent 200-kHz and 6.78-MHz operation in a single-transmitter device," *IEEE Trans. Power Electron.*, vol. 31, no. 7, pp. 5018-5029, Jul. 2016.

[12] H. Hu and S. V. Georgakopoulos, "Multiband and broadband wireless power transfer systems using the conformal strongly coupled magnetic

resonance method," *IEEE Trans. Ind. Electron.*, vol. 64, no. 5, pp. 3595-3607, May 2017.

[13] Z. Pantic, K. Lee and S. M. Lukic, "Multifrequency inductive power transfer," *IEEE Trans. Power Electron.*, vol. 29, no. 11, pp. 5995-6005, Nov. 2014.

[14] F. Liu, Y. Yang, Z. Ding, X. Chen and R. M. Kennel, "A multi-frequency superposition methodology to achieve high efficiency and targeted power distribution for multi-load MCR WPT system," *IEEE Trans. Power Electron.*, vol. 33, no. 10, pp. 9005-9016, Oct. 2018.

[15] F. Liu, Y. Yang, Z. Ding, X. Chen and R. M. Kennel, "Eliminating cross interference between multiple receivers to achieve targeted power distribution for a multi-frequency multi-load MCR WPT system," *IET Power Electron.*, vol. 11, no. 8, pp. 1321-1328, Jun. 2018.

[16] W. Liu, J. Zhang, and R. Chen, "Modelling and control of a novel zero-current-switching inverter with sinusoidal current output," *IET Power Electron.*, vol. 9, no. 11, pp. 2205-2215, Sep. 2016.

[17] Z. Zhang, K. T. Chau, C. Qiu, and C. Liu, "Energy encryption for wireless power transfer," *IEEE Trans. Power Electron.*, vol. 30, no. 9, pp. 5237-5246, Sep. 2015.

[18] J. Deng, W. Li, T. D. Nguyen, S. Li and C. C. Mi, "Compact and efficient bipolar coupler for wireless power chargers: design and analysis," *IEEE Trans. Power Electron.*, vol. 30, no. 11, pp. 6130-6140, Nov. 2015.

[19] Z. Zhang and K. T. Chau, "Homogeneous wireless power transfer for move-and-charge," *IEEE Trans. Power Electron.*, vol. 30, no. 11, pp. 6213-6220, Nov. 2015.

[20] C. C. Mi, G. Buja, S. Y. Choi and C. T. Rim, "Modern advances in wireless power transfer systems for roadway powered electric vehicles," *IEEE Trans. Ind. Electron.*, vol. 63, no. 10, pp. 6533-6545, Oct. 2016.

[21] C. Jiang, K. T. Chau, T. W. Ching, C. Liu and W. Han, "Time-division multiplexing wireless power transfer for separately excited DC motor drives," *IEEE Trans. Magn.*, vol. 53, no. 11, pp. 1-5, Nov. 2017.

[22] M. Sato, G. Yamamoto, D. Gunji, T. Imura, and H. Fujimoto, "Development of wireless in-wheel motor using magnetic resonance coupling," *IEEE Trans. Power Electron.*, vol. 31, no. 7, pp. 5270-5278, Jul., 2016.

[23] R. Mai, Y. Liu, Y. Li, P. Yue, G. Cao and Z. He, "An active-rectifier-based maximum efficiency tracking method using an additional measurement coil for wireless power transfer," *IEEE Trans. Power Electron.*, vol. 33, no. 1, pp. 716-728, Jan. 2018.